

ESTIMATION OF DIELECTRIC RECOVERY OF FAST OPENING COMMUTATING SWITCHES AFTER SHORT TIME ARCS

K. NIAYESH*, A. USLAND

Department of Electric Energy, Norwegian University of Science and Technology (NTNU), Trondheim, Norway

* kaveh.niayesh@ntnu.no

Abstract. Ultra-fast opening mechanical switches are proposed as key components for medium-voltage DC circuit breakers, enabling rapid fault current commutation to a parallel capacitor. After arc extinction in the commutating switch, the gas-filled gap is exposed to rapidly rising transient voltages, and the success of commutation depends on fast dielectric recovery. This paper presents a method to estimate the arc temperature at the time of arc extinction and its subsequent decay after full current interruption in a fast-elongating arc with short arcing times. A modified Lowke model, accounting for arc thermal inertia, is used to track the evolution of arc temperature and radius from arc initiation up to arc extinction. Post-extinction gas temperature decay is modeled using heat transfer in a simplified cylindrical geometry. Finally, the dielectric breakdown voltage of the gap is estimated via critical field theory, accounting for temperature-dependent breakdown fields.

Keywords: short time arcs, fast opening switches, dielectric recovery.

1. Introduction

Fast opening switches have been identified as a crucial component in several proposed DC circuit breaker designs [1–3], where a fast elongating switching arc with a sufficiently high arcing voltage [4] is created in order to facilitate commutation of the arc current to other parallel branches, such as a semiconductor switching component [5] or a non-linear current controlled impedance (such as a PTC resistive element [6]) or even to a linear impedance (such as a capacitor [7], or a combination of inductor and capacitors). In some configurations, to facilitate the current commutation process, an active current injection is used, or even at higher voltage ratings, a series power electronics component is employed. Adding any component to the whole circuit breaker system results in an increase of its complexity and consequently its cost, therefore, a DC circuit breaker with minimum necessary components is the preferred solution.

One of the recently proposed DC circuit breaker configurations for medium voltage applications suggests using a fast mechanical switch in parallel to an appropriately dimensioned capacitor [7]. In this method, the commutating switching gap is exposed to the transient voltage generated over the parallel capacitor after the current commutation is completed. As the targeted arcing times in the commutating switch need to be as short as possible to avoid any excessive degradation of the contact system, the gap length at the time of current commutation is in the range of a few millimeters. Given that an electric arc—even with very short arcing durations—constitutes a thermal gas discharge with elevated temperatures, and that the dielectric breakdown strength of the gas is strongly dependent on its temperature [8, 9], this paper examines the temporal evolution of the temperature within

the short commutating gap up to the instant of complete current commutation, as well as its subsequent decay following arc extinction, in order to estimate the dielectric recovery strength of the switching gap, which must reestablish more rapidly than the voltage rise across the parallel capacitor.

For this purpose, a simple arc model is developed to estimate the arc temperature and its radius at the time of arc extinction accounting for arc thermal inertia. Decay of the temperature of the hot gas filling the switching gap in the post-arc period is considered applying the heat transfer. The calculated temperature profile of the hot gas column, together with the switching gap length, is used to estimate the dielectric recovery of the switching gap with varying arcing time, initial arc current, and opening velocity.

2. Simplifying assumptions

Fast-opening switches can be implemented in various ways, most commonly using an electrodynamic mechanism—known as the Thomson drive—which achieves opening velocities of up to several tens of meters per second [10]. The current-carrying contacts are configured as a set of sliding contacts, where their separation initiates an arc. When integrated with a properly designed parallel branch, the current begins to decrease immediately after separation.

Fig. 1 illustrates a simplified contact configuration typical of fast-opening switches. Although the switching arc exhibits highly dynamic and complex spatial profiles, a short arcing time generally results in a gap length of only a few millimeters at the moment of arc extinction. For the purposes of this study, the arc is idealized as having a simple cylindrical shape. The switch opening velocity is treated as a key parameter

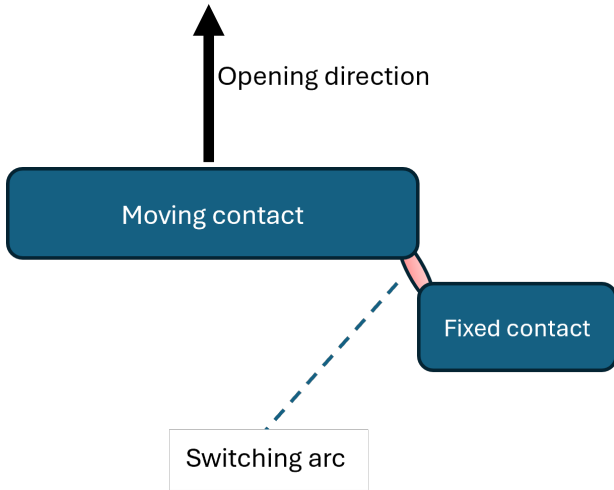


Figure 1. Simplified sliding contact configuration.

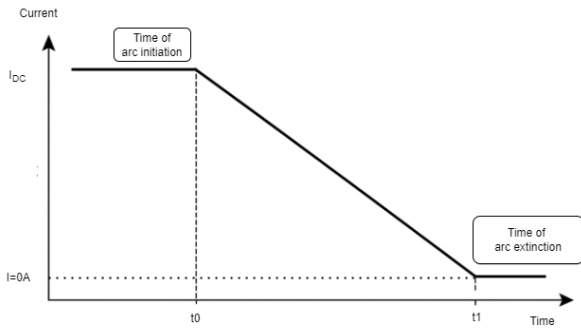


Figure 2. Simplified current waveform used for simulations.

influencing the dielectric recovery following the extinction of the commutating arcs. It is assumed that the gap length increases linearly with time.

In addition, depending on the other components parallel to the mechanical switch, the current could have different decay profiles. In this study, as another simplification, the current waveform is assumed to be as shown in Fig. 2, where it starts at an initial DC current value, I_{DC} , after initiation of the arc by contact separation at t_0 , the current flowing through the switch starts to decline, and at t_1 , it is fully commutated to the parallel branch, so that the arc gets extinguished. The arcing time, i.e., $t_1 - t_0$, and the initial DC current, I_{DC} , are two parameters used to explore dielectric recovery behavior of the short commutating arcs in this paper.

3. Modeling

To estimate the dielectric recovery of commutating switching arcs in fast-opening switches, the arc temperature evolution is first modeled until the arc is extinguished. The arc is assumed to have a cylindrical shape, characterized by a core temperature and a radius. After arc extinction, heat transfer analysis is performed to track the evolution of the temperature

distribution in the hot-gas column during the post-arc period. The resulting temperature profile is then used to estimate the breakdown voltage across the switching gap.

3.1. Switching arc model

In this study, a modified Lowke formulation is employed to model the switching arc. The Lowke model [11] is a stationary approach in which the arc column is assumed to be cylindrical, characterized by a core temperature and a core radius, with a parabolic radial temperature profile. The arc current is used as the primary input parameter. The model has been successfully used to describe the experimental arc behavior in some other studies [12]. However, since the model does not incorporate the temporal evolution of the arc, it cannot accurately predict the arc column temperature near current zero. Instead, it relies solely on the balance between the input and output power of the arc. When applied with the input current waveform shown in Fig. 2, the model predicts unrealistically low temperatures for the gas in the switching gap at the moment of arc extinction, as the instantaneous arc current alone governs the arc temperature and radius.

To account for the dynamic behavior of the switching arc resulted from its thermal inertia, the stationary model has been changed in such a way that the difference between the input and output powers to the arc would result in a change of its internal energy, which will then be reflected in its temperature and radius.

$$\rho c_p \frac{dT}{dt} = \frac{I^2}{\sigma(\pi r^2)^2} - \frac{4kT}{r^2} - U \quad (1)$$

where ρ , c_p , σ , k , T and r are the density, the specific heat, the electric conductivity, the thermal conductivity, the core temperature and the radius of the arc column. I is the current flowing through the arc. U is the radiated power per cubic meter of hot gas per steradian, which can be expressed as [11]:

$$U = \frac{2\beta T^4}{r} \epsilon \quad (2)$$

where β is the Stefan-Boltzmann constant, ϵ a radiation coefficient, which is dependent on the pressure and arc radius and material type. For air, it can be estimated as [11]:

$$\epsilon = 1 - e^{-0.07(pr)^{0.6}} \quad (3)$$

If no time dependence is considered, the left-hand side of (1) becomes zero, and (1) will be reduced to the stationary formulations given in [11]. Inclusion of the change of the internal energy of the arc allows for accounting the impact of the thermal inertia of the arc, which would be of particular importance in case of fast arc current changes, as the case investigated in this study. Adding the thermal inertia part to the power balance has also been used in some earlier studies [13] to successfully describe the arc characteristics. In this

formulation, a parabolic temperature profile within the arc column is assumed, and the heat conduction as well as radiation losses, i.e., the second and third terms on the right-hand side of (1), have been taken into consideration.

3.2. Temperature decay after arc extinction

Temperature and radius of the arc at the time of arc extinction calculated using the model described in Section 3.1, are used as initial values in a heat transfer simulation using a commercial multi-physics simulation tool encountering thermal conductivity and heat convection to evaluate the evolution of the temperature profile of the hot gas column filling the switching gap after the arc current is completely commutated to the parallel capacitor, and arc in the mechanical switch is extinguished. The model includes only natural convection and radial conductive forces from hot to cold gases, and the influence of forced convective forces due to gas flow is not included.

3.3. Temperature dependent critical electric field

Previous studies have demonstrated that the critical electric field depends on temperature in hot gases. In [8], the reduced critical electric field for air is reported for temperatures up to 6000 K. The electrical conductivity of air begins to increase significantly around 6000 K and reaches very high values near 8000 K [14]. The concept of electrical breakdown caused by impact ionization is, therefore, not applicable for temperatures larger than 6000 K as the main charge generation is the thermal ionization of the gas. On the other hand, assuming a constant critical electric field for temperatures above 6000 K, as suggested in [9], would falsify the dielectric recovery estimations of the gap, in particular, in case of larger initial currents, as the estimated arc temperature at the time of current extinction is in the range where high conductance of the air is expected. To rectify this problem, the concept of critical electric field is extended for higher temperatures, where the thermal runaway of the hot gas channel results in re-establishment of the arc channel (re-ignition). For this purpose, a critical current density, J_{critical} , is used to calculate the critical electric field as $\frac{J_{\text{critical}}}{\sigma}$. The measurements in [15] indicate a range of 10^6 to $10^7 \frac{\text{A}}{\text{m}^2}$ for the critical current density that leads to thermal runaway in the air based on post arc current measurements and estimates of the cross section of the arc. With this assumption, the critical electric field continues to decrease beyond 6000 K. For temperatures above 8000 K, the gas channel is unable to sustain any voltage due to its high conductivity, causing the critical electric field to become negligible (see Fig. 3). The solid line in the figure, representing data up to 6000 K, is taken from [8], while the dashed line beyond 6000 K is an extrapolation based on the conductivity behavior of the air [14] and a critical current density of $5 \cdot 10^6 \frac{\text{A}}{\text{m}^2}$.

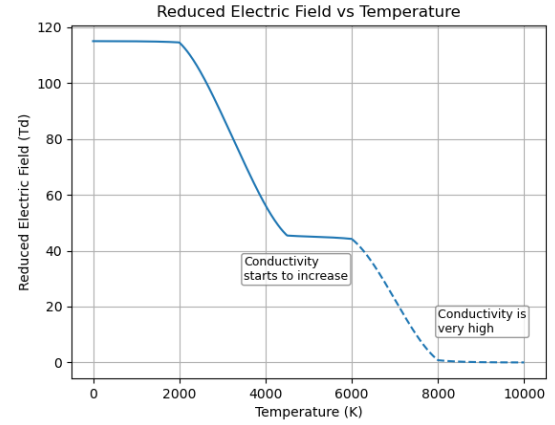


Figure 3. Reduced critical electric field for air at atmospheric pressure as a function of its temperature. The solid line is taken from [8] and the dashed line is the estimation based on increased conductivity of the gas and a critical current density of $5 \cdot 10^6 \frac{\text{A}}{\text{m}^2}$.

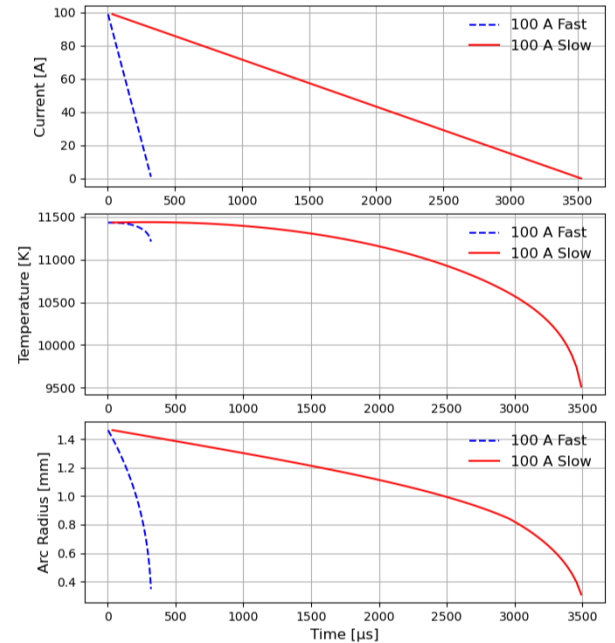


Figure 4. Current, core temperature and radius of the arc with starting current of 100 A and two different arcing times, i.e., $300 \mu\text{s}$ (fast) and $3500 \mu\text{s}$ (slow).

The breakdown voltage of the switching gap after arc extinction field can be calculated using the reduced critical electric field and the particle number density in the gas, integrated over the length of the switching gap.

4. Results and Discussion

4.1. Arc temperature and radius evolution

In this section, the arc temperature and arc radius profiles for different combinations of parameters are reported, including the initial arc current, I_{DC} and the arc duration, $t_1 - t_0$. The calculations are based on the model described in Section 3.1.

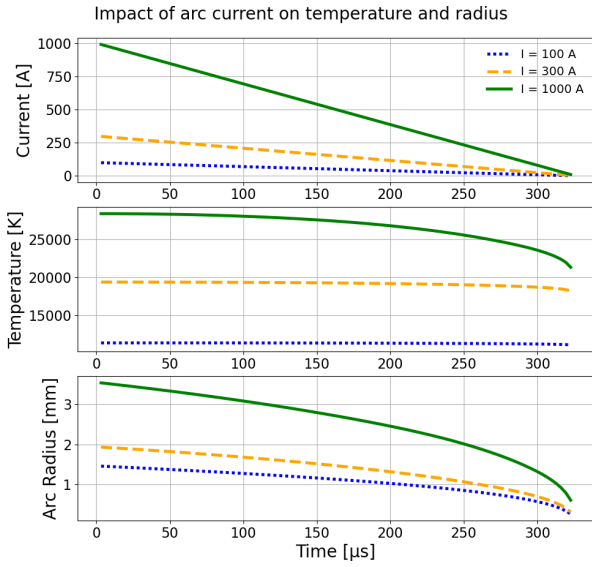


Figure 5. Current, core temperature and radius of the arc with different starting currents, i.e., 100 A, 300 A and 1000 A and the same arcing times of 350 μs .

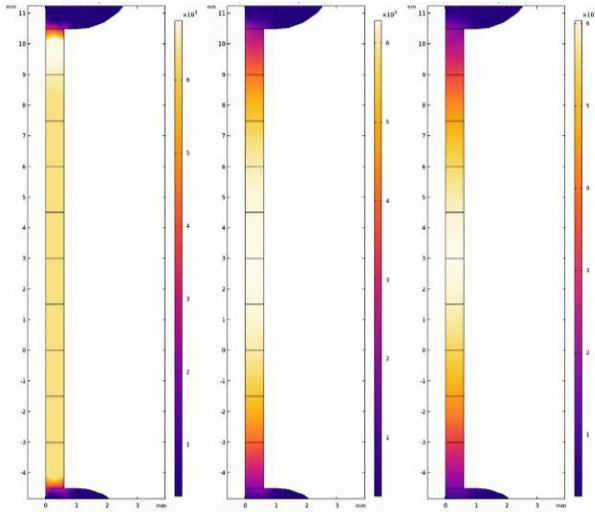


Figure 6. Example of arc temperature profile evolution after arc extinction for a starting arc current of 100 A, arcing time of 3500 μs and at different times after arc extinction, i.e., 10 μs , 50 μs and 100 μs .

The impact of the arc duration on the arc core temperature and arc radius is shown in Fig. 4, where the arc core temperature and arc radius for the same starting DC current of 100 A with different arc durations of 300 μs and 3500 μs are depicted. It seems that the thermal inertia of the arc plays a more pronounced role in case of shorter arcing times resulting in higher temperatures at the time of arc extinction. The arc radius is, however, almost independent of the arc duration.

The role of the initial arc current on the arc temperature and arc radius at the time of arc extinction is shown in Fig. 5. For an arc duration of 350 μs , the temperature and radius profiles of the arc are presented for three different initial arc currents: 100 A,

300 A and 1000 A. The arc temperature at the time of arc extinction shows a strong dependence on the initial arc current, increasing from approximately 11,300 K to over 20,000 K. In contrast, the arc radius at the time of arc extinction exhibits significantly less sensitivity to the initial current, varying only slightly—from about 0.4 mm to around 0.6 mm—even when the initial current is increased tenfold.

4.2. Temperature decay after arc extinction

After the arc current is ceased to zero, there will be no active heating of the hot gas column filling the gap between two electrodes. Due to the heat transfer, the hot gas temperature starts to decay. In the simulation performed to estimate the temperature decay of the hot gas column, the thermal conductivity near electrodes has also been considered.

A typical temperature distribution of the hot gas column at different times is shown in Fig. 6. Even though the arc column temperature is around 9000 K at the time of arc extinction, see Fig. 4, the temperature decays significantly within a few tens of μs . The temperature near electrodes seems to be lower because of a more efficient heat transfer near the electrodes. This results in a range of temperatures along the hot gas column. In this example, after around 200 μs , the gas temperature becomes lower than 2000 K, indicating a cold gas like behavior. It seems that this will be the case for different initial currents as shown in Fig. 7. Even though the temperature at the moment of arc extinction depends strongly on the initial current, it decreases rapidly within a few hundred microseconds.

4.3. Dielectric recovery of the switching gap

The temperature profile of the hot gas is used to estimate the critical electric field along the switching gap at different times after arc extinction. The breakdown voltage can then be calculated as an integral of the critical electric fields over the gap length.

With this background, the role of the initial DC current as well as the arc duration in the dielectric recovery of the short arcs becomes clear as the arc temperature in the post-arc period is highly dependent on both of these two parameters.

The opening velocity plays a dual role in the dielectric recovery of the switching gap. First, it directly influences the gap length at the moment of arc extinction—a key parameter explicitly examined in this study. Second, the opening velocity enhances arc cooling, leading to higher arc voltages and consequently shorter arcing durations. However, this latter effect is only implicitly considered in the present analysis.

Fig. 8 shows the impact of arc duration and opening velocity on the recovery of the switching gap. At higher opening velocities and longer arcing durations, the gap length at the moment of arc extinction tends to be larger, promoting faster dielectric recovery. While shorter arcing times are intuitively seen as beneficial—primarily due to reduced wear on the arcing contacts—

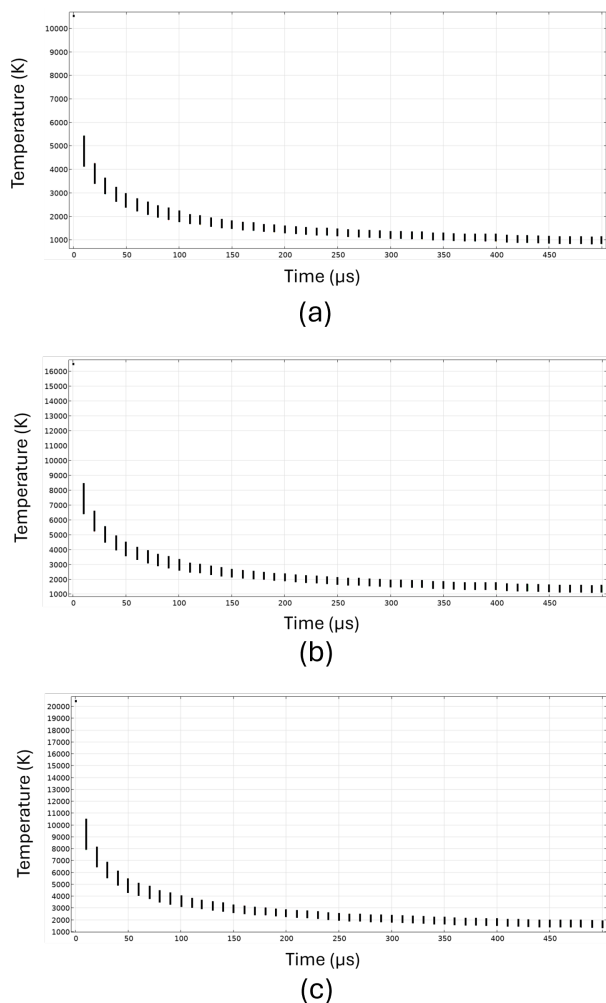


Figure 7. Temperature evolution of the hot gas filling the switching gap after current extinction for arcing time of $300\ \mu\text{s}$ and different initial currents (a) $100\ \text{A}$ (b) $300\ \text{A}$ and (c) $1000\ \text{A}$.

they may inadvertently lead to slower dielectric recovery, as they are associated with smaller gap lengths at current extinction.

Dielectric recovery of a switch opening with different velocities at different initial DC currents is depicted for two different arcing times of $300\ \mu\text{s}$ and $3500\ \mu\text{s}$, in Figs. 9 and 10, respectively.

As previously illustrated (see, for example, Fig. 5), the initial DC current has a pronounced effect on the temperature of the hot gas column at the moment of arc extinction. For currents of $1000\ \text{A}$ and above, the gas temperature significantly exceeds the threshold at which it becomes conductive. Consequently, during the early post-arc phase – within the first few tens of microseconds after arc extinction – the hot gas remains at temperatures above $8000\ \text{K}$. This sustained high temperature leads to negligible dielectric recovery of the switching gap during this period. An increase in opening velocity also has a beneficial effect on dielectric recovery in this case.

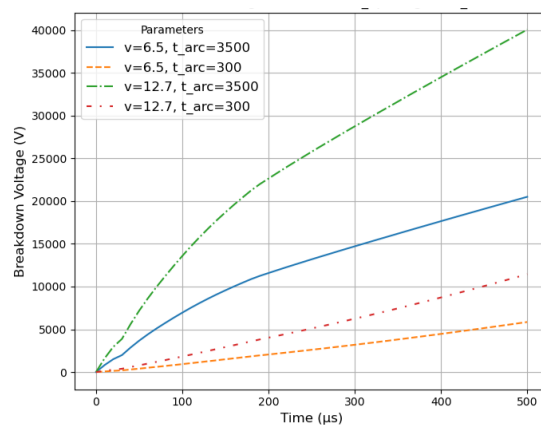


Figure 8. Dielectric recovery of a switching gap with initial DC current of $100\ \text{A}$, for different arcing time and opening velocity combinations.

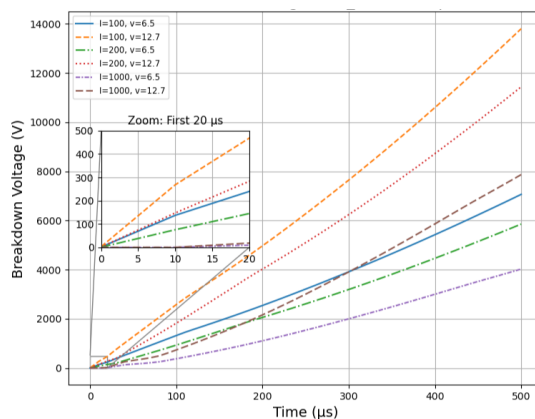


Figure 9. Dielectric recovery of a switching gap with three different initial DC currents, i.e. $100\ \text{A}$, $200\ \text{A}$ and $1000\ \text{A}$, and two different opening velocities, i.e., $6.5\ \text{m/s}$ and $12.7\ \text{m/s}$, and the same arcing time of $300\ \mu\text{s}$.

5. Conclusions

This study presents a simplified thermal model for the development of arc temperature and arc radius, based on the Lowke model and incorporating thermal inertia based on physical parameters. By considering only conduction and radiation, the model effectively demonstrates how the arc duration influences the thermal behavior of the arc. The results show that shorter arcs are more affected by thermal inertia, while longer arcs tend toward steady-state conditions due to increased cooling time and heat dissipation.

The breakdown voltage is shown to increase with arc duration due to greater gap distances, and it is experimentally confirmed that successful current commutation prevents arc re-strikes.

While the developed model provides a useful framework for analyzing the influence of thermal inertia on arc behavior, it represents a simplified approach to a complex physical phenomenon. Several assumptions were made to enable tractable simulations, including

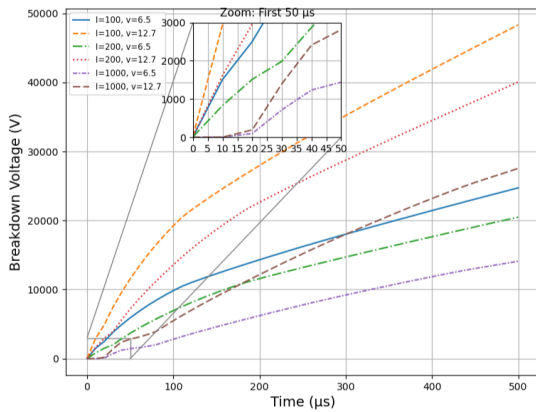


Figure 10. Dielectric recovery of a switching gap with three different initial DC currents, i.e. 100 A, 200 A and 1000 A, and two different opening velocities, i.e., 6.5 m/s and 12.7 m/s, and the same arcing time of 3500 μ s.

the use of a cylindrical arc geometry, the neglect of metal vapor content, and the consideration of only conduction and radiation as cooling mechanisms. These simplifications may affect the quantitative accuracy of the results, particularly under conditions where convection or vapor effects become significant. In addition, the simulation results require experimental verification to confirm their validity. Future work will therefore include targeted experiments and model refinements incorporating additional physical processes and more representative material parameters.

Acknowledgements

This work has received funding from the European Union's Horizon Europe research and innovation project under grant agreement no 101135484 (EU project MISSION). The authors would like to acknowledge interesting discussions with Paul Røren, Silas Gerhard, Fahim Abid and Simon Løvdaal.

References

- [1] X. Pei, O. Cwikowski, D. S. Vilchis-Rodriguez, et al. A review of technologies for MVDC circuit breakers. In *IECON 2016-42nd Annual Conference of the IEEE Industrial Electronics Society*, pages 3799–3805. IEEE, 2016. doi:10.1109/IECON.2016.7793492.
- [2] K. Niayesh. *Green HV Switching Technologies for Modern Power Networks*, volume 236. IET, 2023.
- [3] R. P. Smeets and N. A. Belda. High-voltage direct current fault current interruption: A technology review. *High Voltage*, 6(2):171–192, 2021. doi:10.1049/hve2.12063.
- [4] A. Kadivar and K. Niayesh. Effects of fast elongation on switching arcs characteristics in fast air switches. *Energies*, 13(18):4846, 2020. doi:10.3390/en13184846.
- [5] M. Steurer, K. Frohlich, W. Halaus, and K. Kaltenecker. A novel hybrid current-limiting circuit breaker for medium voltage: principle and test results. *IEEE transactions on power delivery*, 18(2):460–467, 2003. doi:10.1109/TPWRD.2003.809614.
- [6] W. Halaus and K. Frohlich. Ultra-fast switches—a new element for medium voltage fault current limiting switchgear. In *2002 IEEE Power Engineering Society Winter Meeting. Conference Proceedings (Cat. No. 02CH37309)*, volume 1, pages 299–304. IEEE, 2002. doi:10.1109/PESW.2002.985002.
- [7] D. Jovicic. Fast commutation of dc current into a capacitor using moving contacts. *IEEE Transactions on Power Delivery*, 35(2):639–646, 2020. doi:10.1109/TPWRD.2019.2919725.
- [8] H.-J. Jang, Y.-H. Oh, K.-D. Song, and Y.-I. Kim. Prediction of reduced critical electric field strength of hot dry air in the temperature range 300–5000 K at 0.1 MPa for medium-voltage switchgear. *AIP Advances*, 10(4), 2020. doi:10.1063/1.5145146.
- [9] J. Nan, G. Chen, and I. O. Golosnoy. Analysis of breakdown mechanisms in heated short air gaps during contact opening in compact DC circuit breakers. In *2024 IEEE 69th Holm Conference on Electrical Contacts (HOLM)*, pages 1–8. IEEE, 2024. doi:10.1109/HOLM56222.2024.10768674.
- [10] A. Kadivar and K. Niayesh. Practical methods for electrical and mechanical measurement of high speed elongated arc parameters. *Measurement*, 55:473–486, 2014. doi:10.1016/j.measurement.2014.05.017.
- [11] J. Lowke. Simple theory of free-burning arcs. *Journal of physics D: Applied physics*, 12(11):1873, 1979. doi:10.1088/0022-3727/12/11/016.
- [12] P. M. Røren and K. Niayesh. Switching arc characteristics at load currents in air and a fluoroketone–air mixture. *IEEE Transactions on Plasma Science*, 52(5):1815–1821, 2024. doi:10.1109/TPS.2024.3418141.
- [13] T. Christen and M. Seeger. Current interruption limit and resistance of the self-similar electric arc. *Journal of applied physics*, 97(10), 2005. doi:10.1063/1.1913802.
- [14] A. D'angola, G. Colonna, C. Gorse, and M. Capitelli. Thermodynamic and transport properties in equilibrium air plasmas in a wide pressure and temperature range. *The European Physical Journal D*, 46(1):129–150, 2008. doi:10.1140/epjd/e2007-00305-4.
- [15] W. Hauer and X. Zhou. Re-ignition and post arc current phenomena in low voltage circuit breaker. In *ICEC 2014; The 27th International Conference on Electrical Contacts*, pages 1–6. VDE, 2014.